Inorganic Chemistry

Article

pubs.acs.org/IC

Synthesis and Properties of $SmO_{0.5}F_{0.5}BiS_2$ and Enhancement in T_c in $La_{1-y}Sm_yO_{0.5}F_{0.5}BiS_2$

Gohil Singh Thakur,[†] Ganesan Kalai Selvan,[‡] Zeba Haque,[†] Laxmi Chand Gupta,[†,§] Saroj Lochan Samal,[⊥] Sonachalam Arumugam,[‡] and Ashok Kumar Ganguli*[,†,∥]

[†]Solid State and Nano Research Laboratory, Department of Chemistry, Indian Institute of Technology, New Delhi 110016, India

[‡]Centre for High Pressure Research, School of Physics, Bharathidasan University, Tiruchirapalli 620024, India

[⊥]Department of Chemistry, National Institute of Technology, Rourkela, Odisha 769008, India

Supporting Information

ABSTRACT: The crystal structure and properties of a new member of the oxybismuth sulfide family $SmO_{0.5}F_{0.5}BiS_2$ are reported here. The compounds $SmO_{1-x}F_xBiS_2$ (x = 0.0 and 0.5) are isostructural with $LaOBiS_2$ and crystallize in the $CeOBiS_2$-type structure ($P4/nmm$). Sm substitution in $LaO_{0.5}F_{0.5}BiS_2$ ($La_{1-y}Sm_yO_{0.5}F_{0.5}BiS_2$) leads to a gradual decrease in the a-lattice constant; however, the c-lattice constant does not show such a gradual trend. Enhancement in T_c is achieved upon partial substitution of La by the smaller Sm ion. A maximum $T_c \sim 4.6$ K was observed for composition with y = 0.8. Disobeying this trend, T_c disappears unexpectedly in the composition $SmO_{0.5}F_{0.5}BiS_2$ (y = 1.0). Both the undoped and F-doped (x = 0.0 and 0.5) compounds are paramagnetic, exhibiting semiconducting behavior down to 2 K.

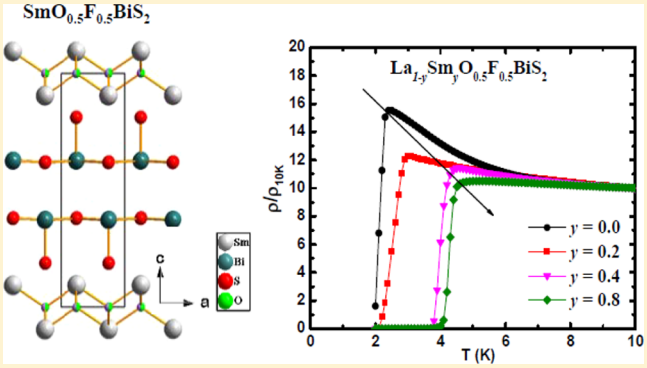

INTRODUCTION

Research in inorganic materials throws up unprecedented structures with unusual properties. The persistence of scientists carrying out exploratory research is challenging amidst dwindling recognition to this genre of scientists. Compounds like Gd_2Cl_3,[1] $NaMo_4O_6$,[2] $YBa_2Cu_3O_7$,[3] K_3C_{60},[4] $TlCa_2Ba_2Cu_2O_8$,[5] and $CaCu_3Ti_4O_{12}$,[6] are compositions that rarely can be designed but were synthesized by the unparalleled intuition (read ingenuity) and labor of solid-state scientists that occasionally rewarded them with footprints for unusual material properties, like high-temperature superconductivity, colossal magnetoresistance, unusually high dielectric constant, negative index of refraction, etc. This Article follows from our work related to a recent class of superconductors, $Bi_4O_4S_3$ and $LnOBiS_2$, that have some structural similarity to the important LnOFeAs class of superconductors.[7−10] For example, both of these systems crystallize in the same space group ($P4/nmm$), they have layered structure with a charge reservoir layer (LnO) and a superconducting layer (BiS_2, Fe−As), their parent phases are semiconducting or poorly conducting, and, most importantly, they become superconducting upon electron doping (doping F^- for O^{2-} or a tetravalent ion for Ln).[9−17] Superconductivity by fluorine doping in $LaO_{1-x}F_xBiS_2$ was first reported by Mizuguchi et al. ($T_c \sim 2.5$ K;[9] $T_c \sim 10$ K could be achieved by high-pressure synthesis).[9] Superconductivity in $LnO_{1-x}F_xBiS_2$ with Ln = Ce, Pr, Nd, and Yb also followed soon after.[10−16] T_c is enhanced by chemical pressure[18−20] or external applied pressure,[22−27] as observed for LnOFeAs;[28] for example, in $LnO_{1-x}F_xBiS_2$, a slight enhancement in T_c has been reported by substituting Se at the S sites or by intermixing rare-earth ions.[18−21] Hole doping via alkali-earth-metal substitution at the Ln site did not yield superconductivity.[22,29] This is in contrast to what is observed in LnOFeAs, where hole doping also induces superconductivity.[30−32] The electronic structure of these chalcogenides is comparable to that of pnictides and is greatly influenced by doping.[33,34] Their bands near the Fermi level consist of states predominantly arising from Bi (6p) and S (3p), and therefore the Bi−S layers are responsible for superconductivity in these materials, while the LnO layer serves as the charge reservoir layer.[33,34] In this Article, (1) we report the single-crystal synthesis, structure, and properties of a new member, $SmO_{1-x}F_xBiS_2$, which has been found to be nonsuperconducting down to 2 K, and (2) we have systematically investigated the effect of doping smaller Sm ions at La sites in $La_{1-y}Sm_yO_{0.5}F_{0.5}BiS_2$ and observed an enhancement in T_c with Sm substitution.

Special Issue: To Honor the Memory of Prof. John D. Corbett

Received: October 2, 2014
Published: January 15, 2015

DOI: 10.1021/ic5023938
Inorg. Chem. 2015, 54, 1076−1081

EXPERIMENTAL SECTION

Polycrystalline samples of $La_{1-y}Sm_yO_{0.5}F_{0.5}BiS_2$ (y = 0.0−1.0) were synthesized by a solid-state method. Ln_2S_3, preheated Ln_2O_3, LnF_3, Bi_2S_3, Bi, and S were ground well and pelletized in the form of circular disks. These disks were then sealed in evacuated silica tubes and heated at 800 °C for 24 h. The product was again ground, pelletized, and heated at 800 °C for 24 h for better homogeneity. The samples were stable in air but preserved in an Ar-filled glovebox to avoid any unnecessary contamination.

Single crystals of $SmO_{1-x}F_xBiS_2$ were grown using a KCl−CsCl flux method. Polycrystalline $SmO_{1-x}F_xBiS_2$ was used as the charge. Approximately 0.5 g of the compound was mixed with 2.5 g of KCl−CsCl (1:1). The properly mixed powder was sealed in an evacuated silica tube. The tube was heated at 800 °C for 24 h and cooled to 600 °C at a rate of 2 °C/h. Then the furnace was shut off and allowed to cool naturally. The tube was opened in an ambient atmosphere, and the flux was dissolved in distilled water. The product was washed several times with distilled water and finally rinsed with acetone. Many platelike micron-sized (100−500 μm) crystals were obtained, as observed under a microscope. All of the chemical manipulations except for vacuum sealing and washing of crystals were performed in an Ar-filled glovebox (H_2O and O_2 < 0.1 ppm).

The phase purity of all of the samples was checked by a powder X-ray diffraction technique using Cu Kα radiation in a Bruker D8 advance diffractometer. Single-crystal diffraction data sets were collected at room temperature over a 2θ range of ∼4° to ∼60° with 0.5° scans in ω and 10 s/frame exposures with the aid of a Bruker SMART CCD diffractometer equipped with Mo Kα radiation (λ = 0.71073 Å). The data showed a primitive tetragonal lattice, and the intensity statistics indicated a centrosymmetric space group. The reflection intensities were integrated with the *APEX II* program in the *SMART* software package.[35] Empirical absorption corrections were employed using the *SADABS* program.[36] The space group *P*4/*nmm* (No. 129) of the structures was determined with the help of *XPREP* and *SHELXTL 6.1*.[37] The structure was solved by direct methods and subsequently refined on $|F^2|$ with combinations of least-squares refinements and difference Fourier maps. The refinements of $SmO_{0.5}F_{0.5}BiS_2$ converged to R1 = 0.0662 and wR2 = 0.1203 for all data with a goodness of fit of 1.17 and maximum residuals of 3.9 and −2.9 e/Å^3, which were 0.8 and 1.1 Å from Bi sites, respectively. Rietveld refinement analysis was carried out on all of the samples using the *TOPAS* software package.[38]

Magnetization measurements in the temperature range of 2−300 K on single crystals were performed by using a Quantum Design Superconducting Quantum Interference Device (SQUID) and on the polycrystalline samples by a vibrating sample magnetometer (VSM) using a Physical Property Measurement System (PPMS). The resistivity studies in the temperature range of 2−300 K on the polycrystalline samples were carried out by a conventional four-probe method using a Quantum Design PPMS.

RESULTS AND DISCUSSION

1. $SmO_{1-x}F_xBiS_2$ (x = 0.0 and 0.5). The Rietveld-refined powder X-ray diffraction pattern of polycrystalline $SmO_{0.5}F_{0.5}BiS_2$ is shown in Figure 1. Most of the peaks could be easily indexed on the basis of a tetragonal system with $CeOBiS_2$ structure in the *P*4/*nmm* space group. The presence of a small amount (<10%) of Bi_2S_3 secondary phase was also detected, which commonly occurs in these types of samples. The refined lattice parameters were found to be a = 4.0122(5) Å and c = 13.5949(2) Å for x = 0.0 and a = 4.0180(1) Å and c = 13.5291(4) Å for x = 0.5. Crystallographic data obtained from single-crystal analysis for $SmO_{0.5}F_{0.5}BiS_2$ are given in Table 1. The corresponding atomic positions and isothermal displacement parameters are listed in Table 2. The CIF file and anisotropic displacement parameters are provided in the Supporting Information (SI). It may be noted that, because

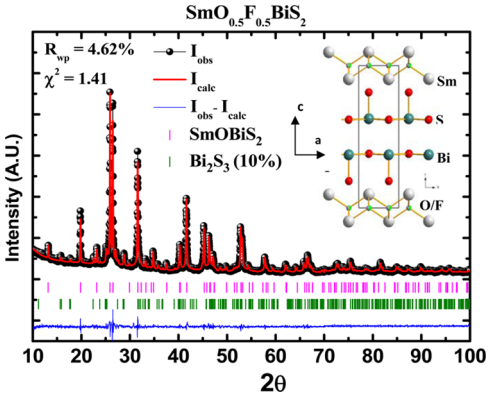

Figure 1. Rietveld refinement studies of the powder X-ray diffraction pattern for $SmO_{0.5}F_{0.5}BiS_2$. Pink and green vertical bars mark the allowed Bragg reflections for the $SmO_{0.5}F_{0.5}BiS_2$ and Bi_2S_3 phases, respectively. The inset shows the crystal structure of $Sm(O,F)BiS_2$.

Table 1. Some Crystal Data and Structural Refinement Parameters for $SmO_{0.5}F_{0.5}BiS_2$

empirical formula	$SmO_{0.5}F_{0.5}BiS_2$
fw (g)	440.95
space group	*P*4/*nmm*
unit cell dimens (Å)	a = 4.018(1), c = 13.534(3)
volume (Å^3)	218.50(1)
density (g/cm^3)	6.70
abs coeff (mm^{-1})	54.28
θ range (deg)	1.5−28.8
index ranges	$-5 \le h \le 3$; $-5 \le k \le 5$; $-18 \le l \le 18$
reflns collected	1096
indep reflns	213
data/param	213/15
GOF on F^2	1.17
final R indices [$I > 2\sigma(I)$]	R1 = 0.0530; wR2 = 0.1143
R indices (all data)	R1 = 0.0662; wR2 = 0.1203
largest diff peak and hole (e/Å^3)	3.94 and −2.93

Table 2. Atomic Coordinates, Wyckoff Positions, and Isotropic Equivalent Displacement Parameters for the $SmO_{0.5}F_{0.5}BiS_2$ Single Crystal[a]

atom	Wyckoff	occupancy	x	y	z	U_{eq} (Å^2)[b]
Sm	2c	1	0.25	0.25	0.0949(2)	0.0196(3)
Bi	2c	1	0.25	0.25	0.6262(1)	0.0205(3)
S1	2c	1	0.25	0.25	0.3799(4)	0.022(4)
S2	2c	1	0.25	0.25	0.8121(4)	0.015(3)
O	2a	0.5	0.75	0.25	0	0.014(3)
F	2a	0.5	0.75	0.25	0	0.014(3)
Bi−S bond length (Å)			equatorial (in-plane, ×4) = 2.8423(2)		axial (×1) = 2.5181(2)	
in-plane S−Bi−S bond angle (deg, ×2)			176.69(4)			

[a]Numbers in parentheses indicate standard deviation. [b]U_{eq} is defined as one-third of the trace of the orthogonalized U^{ij} tensor.

of the similar scattering factors of O and F, their occupancies were not refined and were fixed to nominal values during refinement. $SmO_{1-x}F_xBiS_2$ is isostructural to $LaOBiS_2$ consisting of tetrahedral $Sm_2(O,F)_2$ and fluorite-type BiS_2 layers (inset of Figure 1). The average stoichiometry of the F-doped single-crystal sample was confirmed by EDAX analysis, results of which are given in SI. The relative ratio of Sm:F:Bi:S was found

DOI: 10.1021/ic5023938
Inorg. Chem. 2015, 54, 1076−1081

to be 1:0.39:0.96:2.1. The value of the in-plane or equatorial Bi−S bond length (Bi−S_{eq}) was calculated to be 2.8423(2) Å, and the S−Bi−S bond angle was 176.69(4)°. A comparison of the bond lengths and angles of Sm(O,F)BiS_2 with other F-doped LnOBiS_2 including $Bi_4O_4S_3$ is shown in Figure 2. It is to

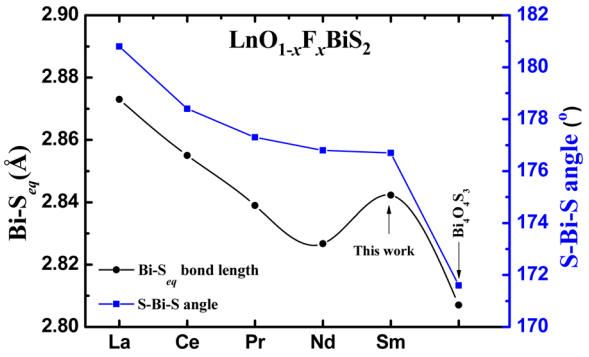

Figure 2. Variation of the in-plane Bi−S bond length (Bi−S_{eq}) and the S−Bi−S angle in known F-doped LnOBiS_2 and $Bi_4O_4S_3$.

be noted that the value of x in each $LnO_{1-x}F_xBiS_2$ is the one that gives the maximum T_c. The values for Ln = La[39] (x = 0.46) and Nd[14] (x = 0.3) were obtained from the single-crystal data reported elsewhere, and for $SmO_{0.5}F_{0.5}BiS_2$, data from the present studies were used. For Ce[10] (x = 0.5), Pr[11] (x = 0.5), and $Bi_4O_4S_3$,[7] the values were obtained from the data reported on polycrystalline samples. Because for the Yb sample no structural refinement data have been reported, the bond lengths and angles could not be calculated. An expected gradual decrease in both the in-plane Bi−S bond distance and the S−Bi−S bond angle is seen with decreasing size of the rare-earth ion from La to Nd. For the Sm system, the Bi−S bond length is anomalously higher than that of Nd, which is a matter of further investigation. Chen et al.[29] studied the effect of local distortion in the Bi−S plane on the superconducting properties of $La_{1-x}M_x(O,F)BiS_2$ (where M = Mg and Ca). They found that a distortion in the Bi−S plane is necessary to enhance the superconductivity in LnOBiS_2. This seems to be true because, upon a decrease in the size of the rare-earth ion, thereby increasing the distortion in the Bi−S plane, T_c is found to increase (from T_c = 2.5 K in La to 5 K in Nd) in $LnO_{1-x}F_xBiS_2$. A similar enhancement in T_c is also observed when two different rare-earth ions are partially substituted, for example, in $Ce_{1-x}Nd_x(O,F)BiS_2$ and $Nd_{1-x}Sm_x(O,F)BiS_2$. T_c increases with an increase in the substitution of a smaller ion up to a certain value.[20,21]

Magnetization measurements in an applied field of 30 Oe carried out on a collection of a large number of tiny single crystals (size ∼100 μm) of composition x = 0.0 and 0.5 exhibit a paramagnetic behavior down to 2 K (Figure 3). These measurements clearly indicate the absence of superconductivity at T > 2 K. The small hump at around 50 K is seen as a result of the freezing of oxygen that might be present in the sample holder or as a result of a slightly poor vacuum in the sample chamber. For the purpose of clarity, the results of the variable-temperature susceptibility (and its inverse) of the polycrystalline sample with x = 0.5 are shown in the low-temperature range (T < 100 K) in Figure 4. The Curie constant C obtained from the Curie−Weiss fit to the χ^{-1} versus T plot is C = 0.47 emu·K/mol and θ_p is −3.6 K. The Sm paramagnetic moment (because there is no other moment carrying species in the

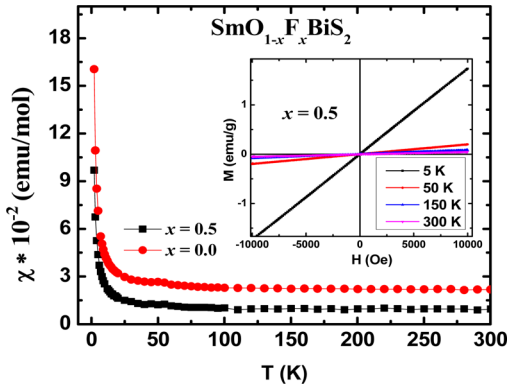

Figure 3. Variable-temperature susceptibility data for $SmO_{1-x}F_xBiS_2$ (the sample comprises a collection of tiny single crystals) measured in a field of 30 Oe (main panel). The inset shows the isothermal magnetization data at different temperatures (5, 50, 150, and 300 K). The small hump at ∼50 K is due to the presence of traces of frozen oxygen impurity.

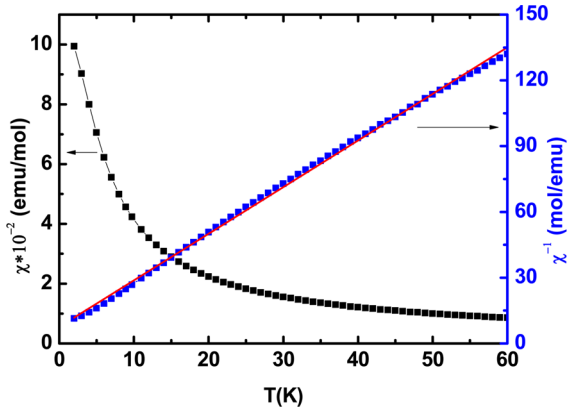

Figure 4. Variable-temperature susceptibility and inverse susceptibility plot for $SmO_{0.5}F_{0.5}BiS_2$ (polycrystalline) in the low-temperature region. The red line shows the Curie−Weiss fit.

material) calculated using this value of C is 0.61 μ_B. The deviation from the magnetic moment expected for the free Sm^{3+} ion (0.84 μ_B) is possibly due to the crystal-field effects. This magnetic moment is consistent with the 3+ ionic state of Sm. The field dependence of magnetization is linear down to 5 K, as shown in the inset of Figure 3, suggesting no magnetic ordering down to 5 K.

The resistivity measured for x = 0.5 on a sintered polycrystalline pellet shows a semiconductor-like behavior similar to that of the undoped compound (x = 0; Figure 5). The resistivity value though decreased upon fluorine doping. We have not seen superconductivity down to 2 K in $SmO_{0.5}F_{0.5}BiS_2$ (see the discussion in the next section). It may be pointed out that other members of this series are known to be superconducting (La, Ce, Nd, Pr, and Yb) with T_c ∼ 2.5−5 K.[15]

$La_{1-y}Sm_yO_{0.5}F_{0.5}BiS_2$. Compositions corresponding to $La_{1-y}Sm_yO_{0.5}F_{0.5}BiS_2$ were synthesized to investigate the possibility of superconductivity by doping La in non-superconducting $SmO_{0.5}F_{0.5}BiS_2$ and also to study the effect of the chemical pressure on T_c. Powder X-ray diffraction patterns of $La_{1-y}Sm_yO_{0.5}F_{0.5}BiS_2$ are presented in Figure 6. The majority of the peaks correspond to the parent LaOBiS_2 phase along with some peaks for impurity phases like Bi_2S_3, Bi_2O_3,

DOI: 10.1021/ic5023938
Inorg. Chem. 2015, 54, 1076−1081

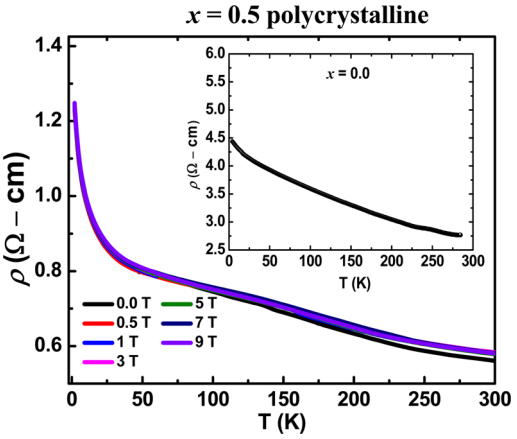

Figure 5. Resistivity versus temperature plots at different magnetic fields for $SmO_{0.5}F_{0.5}BiS_2$ (main panel) and for undoped $SmOBiS_2$ (inset).

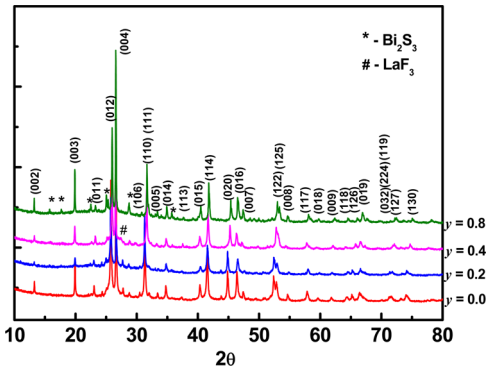

Figure 6. Powder X-ray diffraction patterns for $La_{1-y}Sm_yO_{0.5}F_{0.5}BiS_2$.

BiF_3, and/or LaF_3. Rietveld refinement on all of the compositions was performed to study the crystal structure. The occupancies of La and Sm were refined by constraining their sum to be unity. The occupancies of O and F were fixed to the nominal value. The results of Rietveld refinement and important structural parameters are provided in the SI. The variation of a and c lattice parameters with Sm doping (y) is presented in Figure 7. There is a gradual decrease in the a lattice parameter, as we infer from the shift of the (200) peak toward higher angle (see Figure S5 in the SI). This is expected because Sm has a smaller ionic radius than La. The (004) peak

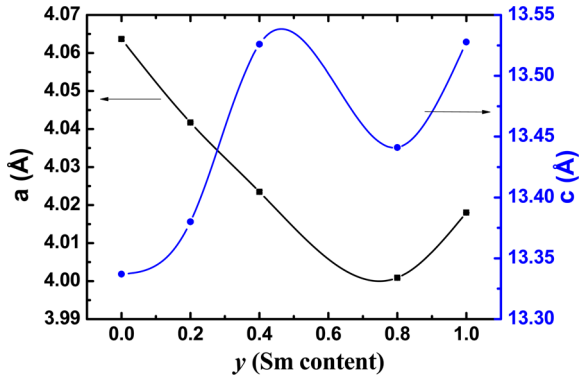

Figure 7. Variation of the lattice parameters a and c with the Sm content (y) for $La_{1-y}Sm_yO_{0.5}F_{0.5}BiS_2$.

does not show a gradual trend as a function of the Sm content (see Figure S5 in the SI). The inferred c lattice parameter also, thus, does not show a gradual (smooth) variation as a function of the Sm content. This type of structural anisotropy is common in layered structures like $Ln(O,F)BiS_2$.[20,21] In contrast to the observation of Kajitani et al.,[21] we do not find a solubility limit of Sm ions at La sites and, hence, La was completely replaced by Sm and the sample with y = 1.0, i.e., $SmO_{0.5}F_{0.5}BiS_2$, could be obtained.

Superconductivity is observed in all of the samples $La_{1-y}Sm_yO_{0.5}F_{0.5}BiS_2$ (y = 0.0, 0.2, 0.4, and 0.8). Figure 8a shows the diamagnetic response in all of these materials. T_c shows an enhancement with an increase in the value of y. A maximum T_c of 4.4 K is observed for y = 0.8. This enhancement in T_c can be attributed to unit cell contraction and local structure distortion, as studied by Chen et al.[29]

The resistivity measurements (Figure 8b) reconfirm the superconducting behavior in these materials. We should point out that, in all of the resistivity plots, a "semiconductor"-like increase in resistivity is observed just before the beginning of the superconducting drop (inset of Figure 8b). This is commonly observed in high-T_c cuprates and in F-doped $LnOBiS_2$ materials. In the upper panel of Figure 9, we show the value of T_c in these materials as measured magnetically and by resistivity. As was already discussed above, the pure Sm sample (y = 1) is nonsuperconducting until 2 K (the limit of our measurement), which means that there may be a critical Sm concentration ($0.8 < y < 1$) that gives a maximum T_c, and the further addition of Sm would suppress the superconducting state. A similar type of study has been very recently reported by Kajitani et al.,[21] in which Sm has been substituted for Nd in $NdO_{0.5}F_{0.5}OBiS_2$ and a maximum T_c is achieved with Sm = 0.6, beyond which the T_c suddenly diminishes. Kajitani et al.[21] also mentioned that there is a solubility limit for Sm in $Nd_{1-x}Sm_xO_{0.5}F_{0.5}BiS_2$ (x = 0.8), but in our study, La and Sm were completely soluble.

STRUCTURE–PROPERTY RELATIONSHIP

Band structure calculations have revealed that the density of state near the Fermi level for these Bi–S superconductors is mainly due to Bi 6p states with only a small contribution from S 3p states.[33,34] The in-plane Bi 6p orbitals are mainly involved in overlap with the S 3p orbitals, and thus the in-plane (ab plane) Bi–S bond lengths and S–Bi–S bond angle seem to be important in inducing and enhancing the superconductivity. Therefore, the local structure in the Bi–S layers is an important parameter for superconductivity in $LnOBiS_2$ vis-à-vis FeAs layers in LnOFeAs superconductors. In order to gain insight, the effect of Sm substitution on the local structure of the Bi–S layers was investigated. The in-plane Bi–S_{eq} distances and in-plane S–Bi–S bond angle were calculated from structural data obtained after Rietveld analysis. The in-plane Bi–S bond lengths largely depend on the a lattice parameter. In the case of Sm doping at La sites, the a lattice parameter decreases gradually, which leads to a decrease in the Bi–S distances, as is evident in the lower panel of Figure 9. Because of the decrease in the Bi–S distance, a better overlap is expected, which seems to enhance T_c. This trend is followed by all of the Sm-doped compositions. The in-plane S–Bi–S angle is also expected to play a significant role in superconductivity. The flatter the bond (~180°), the better the overlap between the Bi 6p and S 3p orbitals. However, as observed by Chen et al.,[29] a little distortion in the Bi–S layer could enhance T_c. A similar trend

DOI: 10.1021/ic5023938
Inorg. Chem. 2015, 54, 1076–1081

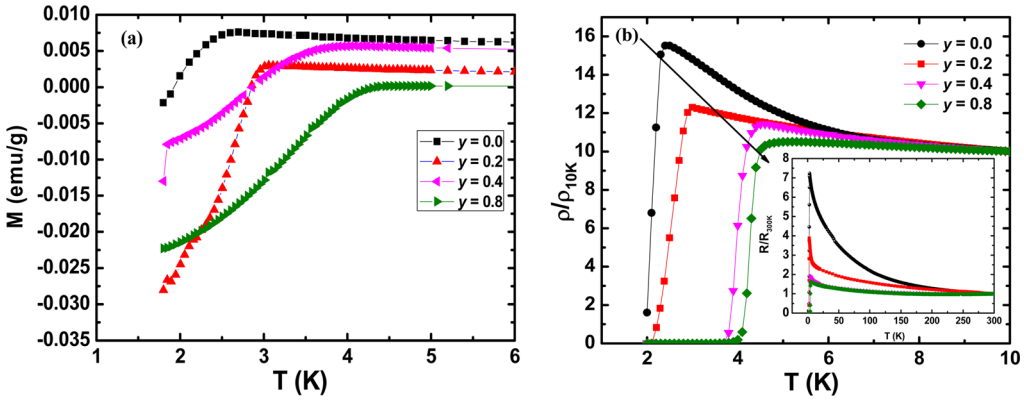

Figure 8. Variable-temperature (a) magnetization and (b) resistivity curves for $La_{1-y}Sm_yO_{0.5}F_{0.5}BiS_2$. The magnetization was measured in zero-field-cooled conditions in a field of 10 Oe. The inset of part b shows resistivity curves up to 300 K.

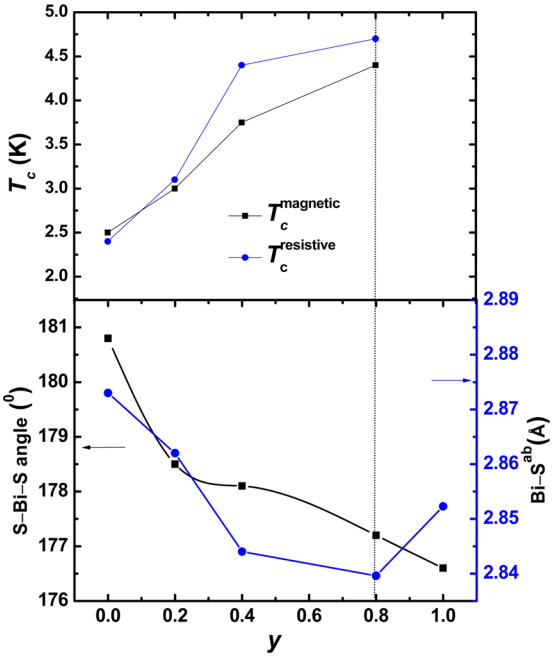

Figure 9. Plot of the variation of T_c obtained from magnetization and resistivity measurements (upper panel) and variation of the Bi−S_{eq} bond length and S−Bi−S angle with y (lower panel) for $La_{1-y}Sm_yO_{0.5}F_{0.5}BiS_2$. The sample $SmO_{0.5}F_{0.5}BiS_2$ (y = 1) does not exhibit superconductivity down to 2 K, the lowest temperature of our measurements.

seems to follow in $La_{1-y}Sm_yO_{0.5}F_{0.5}BiS_2$. In the case of y = 1.0, i.e., the $SmO_{0.5}F_{0.5}BiS_2$ composition, the Bi−S bond length is slightly larger than those of other Sm-doped compositions, which seems to overshadow the favorable effect of distortion in the S−Bi−S bond angle. This may possibly be the reason for the absence of superconductivity in $SmO_{0.5}F_{0.5}BiS_2$, but it needs to be further investigated.

CONCLUSIONS

We have successfully synthesized $SmO_{1-x}F_xBiS_2$, which is a new member of the F-doped $LnOBiS_2$ family. This material is nonsuperconducting and paramagnetic down to 2 K. We have investigated the structure and properties of the Sm-substituted materials $La_{1-y}Sm_yO_{0.5}F_{0.5}BiS_2$ (y = 0.0−1.0) with Sm^{3+} ions smaller in size compared with La^{3+} ions and thus simulating chemical pressure as one effect of substitution. Structural distortion in the Bi−S plane was analyzed. We find that the Bi−S bond lengths decrease with an increase in the doping level of the smaller Sm ion at the La site. We have observed superconductivity in La_{1-y} $Sm_yO_{0.5}F_{0.5}BiS_2$ (y = 0.0−0.8), and we find that T_c is gradually enhanced upon doping Sm at the La site as $y \rightarrow 0.8$. The absence of superconductivity in $SmO_{0.5}F_{0.5}BiS_2$ is anomalous and deserves to be investigated. We also think that a tuning between these parameters via suitable doping or applied pressure could lead to superconductivity in $SmO_{1-x}F_xBiS_2$.

ASSOCIATED CONTENT

Supporting Information

X-ray crystallographic data in CIF format, powder X-ray diffraction patterns, results of Rietveld refinement, and EDAX spectra. This material is available free of charge via the Internet at http://pubs.acs.org.

AUTHOR INFORMATION

Corresponding Author

*E-mail: ashok@chemistry.iitd.ac.in. Phone: 011 2659 1511.

Present Address

[‖]A.K.G.: Director, Institute for Nano Science and Technology Habitat Center, Phase X, sector 64 Mohali, Punjab 160062, India.

Notes

The authors declare no competing financial interest.

[§]L.C.G.: Visiting scientist at Solid State and Nanomaterials Research Laboratory, Department of Chemistry, IIT Delhi, India.

ACKNOWLEDGMENTS

A.K.G. acknowledges DST for financial support. G.S.T. and Z.H. acknowledge CSIR and UGC, respectively, for fellowships. G.K.S. and S.A. acknowledge the Department of Science and Technology (SERB & TSDP), CEFIPRA, New Delhi, UGC (BSR-Meritorious fellowship, SAP, MRP), for their financial support. The authors thank Prof. A. Thamizhavel, TIFR (Mumbai), for providing the PPMS-VSM system for magnetic measurements. The authors at IIT Delhi thank DST for providing the SQUID facility.

DEDICATION

In memory of Prof. John D. Corbett.

DOI: 10.1021/ic5023938
Inorg. Chem. 2015, 54, 1076−1081

REFERENCES

(1) Lokken, D. A.; Corbett, J. D. *Inorg. Chem.* **1973**, *12*, 556−559.
(2) Torardi, C. C.; McCarley, R. E. *J. Am. Chem. Soc.* **1979**, *101*, 3963−3964.
(3) Wu, M. K.; Ashburn, J. R.; Torng, C. J.; Hor, P. H.; Meng, R. L.; Gao, L.; Huang, Z. J.; Wang, Y. Q.; Chu, C. W. *Phys. Rev. Lett.* **1987**, *58*, 908−910.
(4) Hebard, A. F.; Rosseinsky, M. J.; Haddon, R. C.; Murphy, D. W.; Glarum, S. H.; TPalstra, T. M.; Ramirez, A. P.; Kortan, A. R. *Nature* **1991**, *350*, 600−601.
(5) Sheng, Z. Z.; Hermann, A. M. *Nature* **1988**, *332*, 138−139.
(6) Bochu, B.; Deschizeaux, M. N.; Joubert, J. C.; Collomb, A.; Chenavas, J.; Marezio, M. *J. Solid State Chem.* **1979**, *29*, 291−298.
(7) Mizuguchi, Y.; Fujihisa, H.; Gotoh, Y.; Suzuki, K.; Usui, H.; Kuroki, K.; Demura, S.; Takano, Y.; Izawa, H.; Miura, O. *Phys. Rev. B* **2012**, *86*, 220510(R).
(8) Singh, S. K.; Kumar, A.; Gahtori, B.; Shruti, G. S.; Patnaik, S.; Awana, V. P. S. *J. Am. Chem. Soc.* **2012**, *134*, 16504−16507.
(9) Mizuguchi, Y.; Demura, S.; Deguchi, K.; Takano, Y.; Fujihisa, S.; Gotoh, H.; Izawa, H.; Miura, O. *J. Phys. Soc. Jpn.* **2012**, *81*, 114725.
(10) Xing, J.; Li, S.; Ding, X.; Yang, H.; Wen, H. H. *Phys. Rev. B* **2012**, *86*, 214518.
(11) Jha, R.; Awana, V. P. S. *J. Supercond. Novel Magn.* **2014**, *27*, 1−4.
(12) Jha, R.; Kumar, A.; Singh, S. K.; Awana, V. P. S. *J. Supercond. Novel Magn.* **2013**, *26*, 499−502.
(13) Demura, S.; Mizuguchi, Y.; Deguchi, K.; Okazaki, H.; Hara, H.; Watanabe, T.; Denholme, S. J.; Fujioka, M.; Ozaki, T.; Fujihisa, H.; Gotoh, Y.; Miura, O.; Yamaguchi, T.; Takeya, H.; Takano, Y. *J. Phys. Soc. Jpn.* **2013**, *82*, 033708.
(14) Nagao, M.; Demura, S.; Deguchi, K.; Miura, O.; Watauchi, S.; Takei, T.; Takano, Y.; Kumada, N.; Tanaka, I. *J. Phys. Soc. Jpn.* **2013**, *82*, 113701.
(15) Yazici, D.; Huang, K.; White, B. D.; Chang, A. H.; Friedman, A. J.; Maple, M. B. *Philos. Mag.* **2013**, *93*, 673−680.
(16) Awana, V. P. S.; Kumar, A.; Jha, R.; Singh, S. K.; Pal, A.; Shruti, S. J.; Patnaik, S. *Solid State Commun.* **2013**, *157*, 21−23.
(17) Yazici, D.; Huang, K.; White, B. D.; Jeon, I.; Burnett, V. W.; Friedman, A. J.; Lum, I. K.; Nallaiyan, M.; Spagna, S.; Maple, M. B. *Phys. Rev. B* **2013**, *87*, 174512.
(18) Wang, X.-C.; Chen, D.-Y.; Guo, Q.; Yu, J.; Ruan, B.-B.; Mu, Q.-G.; Chen, G.-F.; Ren, Z.-A. http://arxiv.org/abs/1404.7562.
(19) Shao, J.; Liu, Z.; Yao, X.; Zhang, L.; Pi, L.; Tan, S.; Zhang, C.; Zhang, Y. *Europhys. Lett.* **2014**, *107*, 37006.
(20) Kajitani, J.; Omachi, A.; Hiroi, T.; Miura, O.; Mizuguchi, Y. *Physica C* **2014**, *504*, 33−35.
(21) Kajitani, J.; Omachi, A.; Hiroi, T.; Miura, O.; Mizuguchi, Y. http://arxiv.org/abs/1408.2625.
(22) Jeon, I.; Yazici, D.; White, B. D.; Friedman, A. J.; Maple, M. B. *Phys. Rev. B* **2014**, *90*, 054510.
(23) Kotegawa, H.; Tomita, Y.; Tou, H.; Izawa, H.; Mizuguchi, Y.; Miura, O.; Demura, S.; Deguchi, K.; Takano, Y. *J. Phys. Soc. Jpn.* **2012**, *81*, 103702.
(24) Wolowiec, C. T.; Yazici, D.; White, B. D.; Huang, K.; Maple, M. B. *Phys. Rev. B* **2013**, *88*, 064503.
(25) Kajitani, J.; Deguchi, K.; Hiroi, T.; Omachi, A.; Demura, S.; Takano, Y.; Miura, O.; Mizuguchi, Y. *J. Phys. Soc. Jpn.* **2014**, *83*, 065002.
(26) Selvan, G. K.; Kanagaraj, M.; Muthu, S. E.; Jha, R.; Awana, V. P. S.; Arumugam, S. *Phys. Status Solidi RRL* **2013**, *7*, 510−513.
(27) Fujioka, M.; Nagao, M.; Denholme, S. J.; Tanaka, M.; Takeya, H.; Yamaguchi, T.; Takano, Y. *Appl. Phys. Lett.* **2014**, *105*, 052601.
(28) Takahashi, H.; Igawa, K.; Arii, K.; Kamihara, Y.; Hirano, M.; Hosono, H. *Nature* **2008**, *453*, 376−378.
(29) Chen, H.; Zhang, G.; Hu, T.; Mu, G.; Li, W.; Huang, F.; Xie, X.; Jiang, M. *Inorg. Chem.* **2014**, *53*, 9−11.
(30) Wen, H. H.; Mu, G.; Fang, L.; Yang, H.; Zhu, X. *Europhys. Lett.* **2008**, *82*, 17009.
(31) Wu, G.; Chen, H.; Xie, Y. L.; Yan, Y. J.; Wu, T.; Liu, R. H.; Wang, X. F.; Fang, D. F.; Ying, J. J.; Chen, X. H. *Phys. Rev. B* **2008**, *78*, 092503.
(32) Kasperkiewicz, K.; Bos, J. W. G.; Fitch, A. N.; Prassides, K.; Margadonna, S. *Chem. Commun.* **2009**, 707−709.
(33) Shein, I. R.; Ivanovskii, A. L. *J. Expt. Theor. Phys. Lett.* **2012**, *96*, 859.
(34) Morice, C.; Artacho, E.; Dutton, S. E.; Molnar, D.; Kim, H. J.; Saxena, S. S. http://arxiv.org/abs/1312.2615.
(35) *SMART*; Bruker AXS, Inc.: Madison, WI, 1996.
(36) Blessing, R. H. *Acta Crystallogr.* **1995**, *A51*, 33.
(37) *SHELXTL*; Bruker AXS, Inc.: Madison, WI, 2000.
(38) *TOPAS*, version 4.2; Bruker AXS: Karlsruhe, Germany, 2009.
(39) Miura, A.; Nagao, M.; Takei, T.; Watauchi, S.; Tanaka, I.; Kumada, N. *J. Solid State Chem.* **2014**, *212*, 213−17.

DOI: 10.1021/ic5023938
Inorg. Chem. 2015, 54, 1076−1081